

Optimized Design for Illusion Device by Genetic Algorithm

zhengzhong yu (✉ nanfish@jit.edu.cn)

Jinling Institute of Technology

Zhong Yang

Jinling Institute of Technology

yizhi Wang

Jinling Institute of Technology

Xingliu Hu

Jinling Institute of Technology

Xiaomin Tian

Jinling Institute of Technology

Yan Zhang

Jinling Institute of Technology

Research Article

Keywords: illusion device, genetic algorithm, core-shell, single-layered shell

Posted Date: February 4th, 2021

DOI: <https://doi.org/10.21203/rs.3.rs-154259/v1>

License:   This work is licensed under a Creative Commons Attribution 4.0 International License.

[Read Full License](#)

Optimized design for illusion device by genetic algorithm

Zhenzhong Yu*, Zhong Yang, Yan Zhang*, Yizhi Wang, Xingliu Hu & Xiaomin Tian

School of Intelligence Science and Control Engineering, Jinling Institute of Technology, Nanjing,
211169, China.

The optimized design for the illusion device is studied based on the genetic algorithm. For an electrically small target, a core-shell illusion device by optimizing the material and geometrical parameters of the covering shell can achieve the equivalent scattering, in which the monopolar and dipolar modes are dominant. With the increase of the device size, more scattering terms become obvious, and the ability of the single-layered shell to manipulate the scattering is very limited. For a target with dimension compared with the wavelength, we construct a concentric multi-layered device made of isotropic and homogeneous materials. The full-wave simulations are carried out to demonstrate the illusion performance of the optimized multilayer. The physical explanation is given that all scattering modes of the multi-layered illusion device after optimization approach to that of the target.

Transformation optics (TO) can be used to design a wide variety of functional optical devices including invisibility cloak¹⁻³, illusion optical device⁴⁻¹⁰, and so on. Based on the coordinate transformation, the material of these intriguing devices are highly complex, being inhomogeneous and anisotropic in the components of the permittivity and permeability tensors. Y. Lai et al. first proposed the concept of illusion optics which can make an object look like another one⁴. The

* Corresponding author, email: nanfish@jit.edu.cn

* Corresponding author, email: yan04749@jit.edu.cn

illusion devices have many electromagnetic manipulation functionalities, as follows. A conversion device can transform a PEC object into a virtual dielectric object with arbitrary material parameters⁵. A superscatterer can make an object look like a bigger target⁶, but a shrinking device can transform an object virtually into a small-size object⁷. A source illusion device can transform one source into many⁸. Similarly, a ghost illusion device can create multiple virtual ghost images of the original object⁹. The illusion devices mentioned above have aroused great interest because they may lead to many unprecedented applications. However, material parameters derived from TO are extremely complex, even requiring negative index materials.

Another approach to achieving the electromagnetic illusion is based on the scattering cancellation mechanism which was first proposed by Alu and was originally used to design the invisibility cloak¹¹⁻¹³. In 2015, F. Yang et al. generalized the scattering cancellation method for the design of a spherical illusion device by a single-layered isotropic shell¹⁴. For the cylindrical structure, L. Zhang et al. investigate illusion of inhomogeneous and anisotropic cylinders, respectively^{15,16}. In our previous research, a cylindrical core-shell illusion device composed of isotropic and homogeneous materials was studied. We analyzed in detail what range of shell permittivity may be possible to achieve a certain target, and the physical insight into the parameters' distribution was explained by calculating the dipole moment in the core-shell structure¹⁷. The above illusion devices based on the scattering cancellation commonly use an isotropic coating layer, which can greatly reduce the difficulty of fabrication. However, the illusion effect is limited to the device with dimension much smaller than the wavelength.

For an object with its dimension compared to wavelength, the higher-order scattering modes become evident, which may make the performance of illusion device based on the analytical theory

of the scattering cancellation less effective. Similar problems also appear in the cloaking design. In the previous study, we construct a concentric multi-layered cloak for different-sized concealed targets by optimizing the material and geometrical parameters of each covering layer^{18,19}. In this research of the illusion device, we demonstrate that with optimization of the core-shell structure through genetic algorithm (GA), the scattering of this core-shell structure can be equivalent to a target much smaller than the wavelength. With the increase of the device size, multi-layered illusion device is used to increase the freedom of optimized parameters and has better illusion effect than the simple core-shell structure.

Results

Firstly, we consider an electrically small cylindrical core-shell illusion device made of isotropic materials which is placed in the free space with constitutive parameters (ε_0, μ_0) , shown in the inset of figure 1(a). The radius, permittivity and permeability of the core-shell structure are denoted as $(r_c, \varepsilon_c, \mu_c)$ and $(r_s, \varepsilon_s, \mu_s)$, respectively. This core-shell structure with elaborate design can be disguised as a target cylinder with parameters $(r_t, \varepsilon_t, \mu_t)$. For simplicity, the TE_z polarized plane wave is considered, and only the component of magnetic field in the cylinder axis is non-zero. According to the Mie theory, the scattered magnetic field from the multilayers or the bare target cylinder can be represented in the cylindrical coordinates (r, θ, z) by the sum of Hankel functions of the second kind as²⁰

$$H_z^{sca}(r, \theta) = \sum_{n=-\infty}^{+\infty} c_n H_n^{(2)}(k_0 r) e^{jn\theta} \quad (1)$$

where $k_0 = \omega \sqrt{\mu_0 \varepsilon_0}$ represents the wave number in the free space, and c_n represents the scattering coefficient which can be determined by applying the boundary condition of each layer. In order to compare the far-field scattering distribution between the illusion device and the target object, the

calculation of bistatic scattering width is necessary which is usually represented by²⁰

$$\sigma(\theta) = \frac{4}{k_0} \left| \sum_{n=-\infty}^{+\infty} c_n j^n e^{jn\theta} \right|^2 \quad (2)$$

When the radius of the cylindrical structure is much smaller than the working wavelength, the scattering mainly composed of the $n=0$ and $n=\pm 1$ scattering terms. To achieve a good illusion performance in the quasistatic condition, the scattering coefficient $c_n^{core-shell}$ for the core-shell illusion device and coefficient c_n^{target} for the target cylinder should satisfy the following equation

$$c_n^{core-shell} = c_n^{target}, \quad |n| = 0, 1. \quad (3)$$

Optimization procedure based on GA, which was once used to optimize the multilayered cloak, is applied to achieve the core-shell illusion device. The fitness function f in the GA can be chosen as the sum of the difference of the two scattering coefficients from $n=-1$ to $n=1$, which is described as

$$f = \sum_{n=-1}^1 |c_n^{core-shell} - c_n^{target}| \quad (4)$$

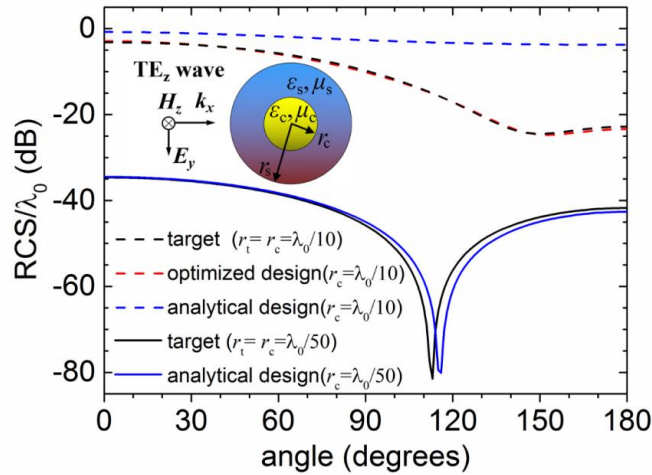


Figure 1. The scattering width normalized by wavelength for the optimized and analytical core-shell design. Two different radii of the core are considered respectively with $r_c = \lambda_0/10$ (dashed lines) and $r_c = \lambda_0/50$ (solid lines). We assume that the radii of core and target are equal, namely $r_i = r_c$. The constitutive parameters of the core and the target are $(3\epsilon_0, 3\mu_0)$ and $(5\epsilon_0, 1.5\mu_0)$, respectively. The inset shows that a TE_Z plane wave is normally incident on a core cylinder coated by a homogeneous isotropic shell.

Given the parameters of the core (r_c, ϵ_c, μ_c) and the target (r_t, ϵ_t, μ_t) in advance, we optimize the parameters of the covering shell (r_s, ϵ_s, μ_s) to achieve the equivalent scattering. In this case, the

fitness function $f(r_s, \varepsilon_s, \mu_s)$ is a function of the shell parameters. GA searches for the optimal shell parameters by approaching the fitness function to the minimum value. In our previous study,¹⁷ the design of the core-shell illusion device is based on the analytical formula method which is only applicable to the case that the device size is far less than wavelength λ_0 , often less than $\lambda_0/15$. To obtain a very similar scattering distribution, the size of the illusion device should be even less than $\lambda_0/50$. Compared with the analytical design, the optimized design based on GA has more degrees of freedom, and greatly widens the size application range of the illusion device. In the following, the analytical method and optimization approach are respectively used to design the shell parameters of the illusion device. We consider that the constitutive parameters of the central core are $(3\varepsilon_0, 3\mu_0)$, that of the target cylinder are $(5\varepsilon_0, 1.5\mu_0)$, and assume that the radii of core and target are equal, namely the radius ratio $\gamma_r=r_t/r_c=1$. In our previous analytical design, contour maps were used to visualize the corresponding relationship between the parameters of the target and the core-shell structure. It can be seen from the contour maps that there are many satisfied parameters of the shell under the condition of parameters given above. If a shell of moderate thickness is selected with $r_s=1.44r_c$, the constitutive parameters of the shell can be calculated as $(1.342\varepsilon_0, -0.3972\mu_0)$ from the analytical formula¹⁷. For the optimization approach, we consider the radius of the core cylinder is $r_c=\lambda_0/10$, and the optimized shell parameters $(r_s, \varepsilon_s, \mu_s)$ are $(1.44r_c, 15.45\varepsilon_0, 6.93\mu_0)$ by minimizing the fitness function. Considering the practical constraints on the constitutive parameters of the shell, the search space of the relative parameters in the optimization process are limited between 1 and 20. Figure 1 shows the far-field scattering widths when a TE_c -polarized plane wave normally incident onto above two types of illusion devices. Three dashed lines in the figure correspond to the case that the radius of the core cylinder is $r_c=\lambda_0/10$, in which the black dashed line is the RCS curve of the

target cylinder, the blue dashed line is the RCS of the core-shell structure based on the analytical formula and the red dashed line is the RCS of the optimized illusion device. It can be found that the optimized illusion device has a similar scattering distribution to that of the target cylinder. However, the scattering of analytical illusion device is significantly different because the analytical design is only applicable when the device size is much smaller than the wavelength. For example, when the size of illusion device is $r_c=\lambda_0/50$, RCS of the analytical illusion device is very close to that of the target, shown by solid lines in figure 1. Full-wave EM simulations with the COMSOL Mutiphysics are carried out to validate the illusion effect when the core cylinder is $r_c=\lambda_0/10$. The total magnetic field simulations of the target and the optimized device, shown in figure 2 (a) and (b), have nearly the same distribution in the exterior region, which verifies the effectiveness of the optimized design for the small target.

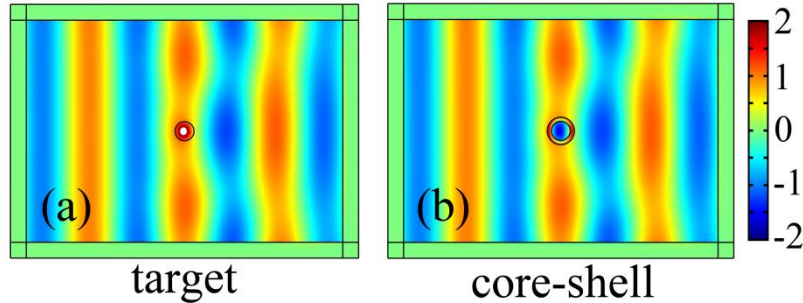


Figure 2. A TE_z polarized plane wave with unit magnitude is incident horizontally from the left side. The z -directed magnetic field distributions of the target (a) and the optimized core-shell illusion device (b) are simulated using COMSOL Mutiphysics. The magnitudes out of the colour bar range are represented by white area.

The above results show that the optimized design of the core-shell illusion device is only applicable to the case that the size of the device is far less than the wavelength. However, with the increase of the device size, more scattering terms become obvious, and the ability of the single-layered shell to manipulate the scattering is very limited. Multilayered structure is needed to increase the freedom of optimized parameters, so that the multilayered illusion device and the target

cylinder may have almost the same scattering coefficients, namely

$$c_n^{multilayer} = c_n^{target}, \quad |n| = 0, 1, 2, 3L \quad (5)$$

We still use the optimization method of GA to design the multilayered illusion device. The fitness function f in the optimization can be chosen as the sum of the difference of all scattering coefficients, which is described as

$$f = \sum_{n=-\infty}^{+\infty} |c_n^{multilayer} - c_n^{target}| \quad (6)$$

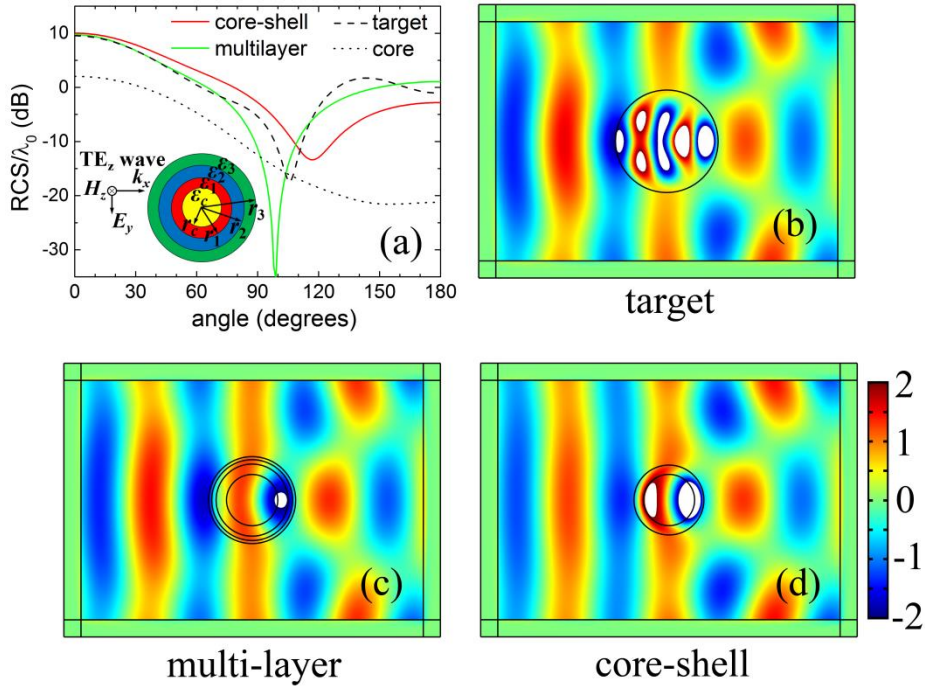


Figure 3. (a) The scattering width normalized by wavelength for the target cylinder with radius $r_t = \lambda_0/2$ (dashed black line), the core cylinder with radius $r_c = \lambda_0/4$ (dotted black line), the optimized multi-layered design (solid green line), and the optimized core-shell design (solid red line). The inset shows that a core cylinder coated by three layers of homogeneous and isotropic materials. The magnetic field distributions of the target (b), the optimized multi-layered illusion device (c), and the optimized core-shell illusion device (d) are simulated using COMSOL Mutiphysics. The magnitudes out of the colour bar range are represented by white area.

In the following, we consider that the constitutive parameters of the central core and the target cylinder are $(2\epsilon_0, \mu_0)$ and $(6\epsilon_0, \mu_0)$, respectively. The radii of the core and the target are $r_c = \lambda_0/4$ and $r_t = \lambda_0/2$, respectively. A 3-layer nonmagnetic shell made of ordinary dielectric materials is used to cover the core cylinder, shown in the inset of figure 3(a). The outer radius and permittivity of each

layer, namely $\{\varepsilon_1, \varepsilon_2, \varepsilon_3, r_1, r_2, r_3\}$, is optimized by GA. Each outer radius is limited to a certain range to ensure a moderate-size shell, and the relative permittivity is constrained between 1 and 20. The optimized parameters for the 3-layer shell are $\varepsilon_1=1.211\varepsilon_0$, $\varepsilon_2=3.086\varepsilon_0$, $\varepsilon_3=6.135\varepsilon_0$, $r_1=0.3513\lambda$, $r_2=0.394\lambda$ and $r_3=0.424\lambda$. For comparison, a single-layered core-shell illusion device is also considered with the optimized parameters of the shell $\varepsilon_s=5.3\varepsilon_0$, and $r_s=0.3407\lambda$. In order to give a full characterization of the scattering by the optimized illusion device, we further investigate the angular distribution of the far-field normalized scattering width (normalized by wavelength), shown in figure 3(a). It can be seen that the scattering distributions of the core and the target are quite different, but after optimization the scattering distribution of the core-shell structure and the multilayer are similar to that of the target. Moreover, the scattering width of the optimized multilayer is closer to that of the target cylinder at most angles, except a small angle range around the 100 degrees. Full-wave electromagnetic simulations are also carried out to visualize the performance of the optimized multilayer and the core-shell structure in comparison with that of target cylinder, shown in figure 3 (b) (c) (d). The total magnetic field distributions of the target and the optimized multi-layered design are almost the same in the outer region. For the optimized core-shell structure, the backscattering is obviously smaller than that of the target. The above results indicate that the optimized 3-layer illusion device can provide more degrees of freedom to achieve a better illusion performance.

Discussion

The reason that quasi-perfect illusion performance can be achieved with only a few optimized layers can be explained as follows. In the GA, the fitness function is determined by the difference between the scattering coefficients of the multi-layered illusion device and the target, denoted by

equation (3). These two kinds of scattering coefficients may be close to each other after optimization. To demonstrate this, the real and imaginary parts of the coefficients at different scattering orders are plotted in figure 4. It can be seen that the first six coefficients c_n ($n = 0\sim 5$) of the target with $r_t = \lambda_0/2$ are dominant and other higher-order coefficients can be negligible. Although the coefficients of the core are quite different from that of the target, the curve of the optimized multilayer almost coincides with that of the target, except $Re(c_5)$ and $Im(c_4)$. All of the first five coefficients ($n = 0\sim 4$) of the core-shell structure deviate a little from that of the target, except the dipolar coefficient ($n = 1$). Therefore, compared with the core-shell design, the optimized 3-layer illusion device has more optimized parameters to achieve a better illusion performance. The physical mechanism for the optimized illusion device is that superposition of each multipolar moment in the core and the multi-layered shell is equal to that of target. When we consider a very small target from which the scattering is dominated by the dipole mode, the mechanism of the core-shell illusion device can be easily explained that the total dipole moments in the core and the covering shell are equivalent to that of the target.

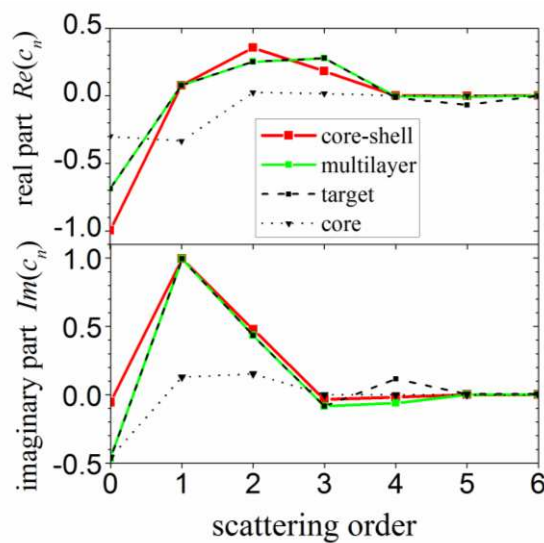


Figure 4. Real and imaginary parts of the Mie scattering coefficients for the optimized 3-layer illusion device at different scattering orders.

In conclusion, we have studied the optimized design for the illusion device with isotropic and homogeneous materials. For an electrically small target, a core-shell structure with the optimized material and geometrical parameters can achieve the equivalent scattering. For a target with dimension compared with the wavelength, we construct an optimized 3-layer structure which has more optimized parameters to achieve a better illusion performance than the core-shell structure. Therefore, it is concluded that the optimized design method can greatly widen the application range of the dimension with the multi-layered illusion device. In comparison, the transformation-based illusion devices use very complex materials, and the scattering-cancellation illusion devices are preferable for particles with small dimension. Our proposed illusion devices take both the advantages of the above two methods, i.e., the transformation-based illusion devices applicable to larger objects and the scattering-cancellation illusion devices using isotropic and homogeneous materials.

Methods

In this paper, genetic algorithm (GA) is used to optimize the cylindrical multi-layered illusion device. GA is an optimization method to search for optimal solution by simulating natural evolution process, which can be used to solve a wide range of real-world problems of significant complexity, including the problems of discontinuous, non-differentiable, and highly nonlinear objective function²¹. Here, we utilize the GA toolbox implemented in the MATLAB software, which is easy to set the range of optimized parameters considered from the practical consideration. GA manipulates a population of artificial chromosomes, which are string representations of solutions to the problem. Each chromosome has a fitness which is a measure of how well the problem is solved.

Starting with a randomly generated population of chromosomes, the GA randomly selects individuals from the current population as parents and carries out a process of fitness-based selection and recombination to produce children for the next generation. After several generations, the population evolves to the optimal solution. For the optimized illusion device of the cylindrical multi-layered structure, GA is used to minimize the fitness function by searching the optimal permittivity and the thickness of the covering layers.

Reference

1. Pendry, J. B., Schurig, D. & Smith, D. R. Controlling Electromagnetic Fields. *Science* **312**, 1780 (2006).
2. Schurig, D. *et al.* Metamaterial Electromagnetic Cloak at Microwave Frequencies. *Science* **314**, 977 (2006).
3. Cai, W. S., Chettiar, U. K., Kildishev, A. V. & Shalaev, V. M. Optical cloaking with metamaterials. *Nature Photon.* **1**, 224 (2007).
4. Lai, Y., Ng, J., Chen, H. Y., Han, D. Z., Xiao, J. J., Zhang, Z. Q. & Chan, C. T. Illusion Optics: the Optical Transformation of an Object into Another Object. *Phys. Rev. Lett.* **102**, 253902 (2009).
5. Jiang, W. X., Ma, H. F., Cheng, Q. & Cui, T. J. Virtual conversion from metal object to dielectric object using metamaterials. *Opt. Express* **18**, 11276 (2010).
6. Yang, T., Chen, H. Y., Luo, X. & Ma, H. Superscatterer: enhancement of scattering with complementary media. *Opt. Express* **16**, 18545 (2008).
7. Jiang, W. X., Cui, T. J., Yang, X. M., Ma, H. F. & Cheng, Q. Shrinking an arbitrary object as one desires using metamaterials. *Appl. Phys. Lett.* **98**, 204101 (2011).
8. Chen, H., Xu, Y., Li, H. & Tomáš, T. Playing the tricks of numbers of light sources. *New J. Phys.* **15**, 093034 (2013).
9. Jiang, W. X., Qiu, C. W., Han, T. C., Zhang, S. & Cui, T. J. Creation of ghost illusion using wave dynamics in metamaterials. *Adv. Funct. Mater.* **23**, 4028 (2013).
10. Zang, X. F. & Jiang, C. Overlapped optics, illusion optics, and an external cloak based on shifting media. *J. Opt. Soc. Am. B* **28**, 1994 (2011).
11. Alù, A. & Engheta, N. Achieving transparency with plasmonic and metamaterial coatings. *Phys. Rev. E* **72**, 016623 (2005).
12. Alù, A. & Engheta, N. Plasmonic materials in transparency and cloaking problems: mechanism, robustness, and physical insights. *Opt. Express* **15**, 3318 (2007).
13. Alù, A., Rainwater, D. & Kerkhoff, A. Plasmonic cloaking of cylinders: finite length, oblique illumination and cross-polarization coupling. *New J. Phys.* **12**, 103028 (2010).
14. Yang, F., Mei, Z. L., Jiang, W. X. & Cui, T. J. Electromagnetic illusion with isotropic and homogeneous materials through scattering manipulation. *J. Opt.* **17**, 105610 (2015).

15. Zhang, L., Shi, Y. & Liang, C. H. Achieving illusion and invisibility of inhomogeneous cylinders and spheres. *J. Opt.* **18**, 085101 (2016).
16. Zhang, L., Shi, Y. & Liang, C. H. Optimal illusion and invisibility of multilayered anisotropic cylinders and spheres. *Opt. Express* **24**, 23333 (2016).
17. Yu, Z. Z., Yang, Z., Zhang, Y., Hu, X. L. & Wang, Y. Z. Physical insights into cylindrical illusion device with isotropic and homogeneous materials. *IEEE Access* **8**, 26468 (2020).
18. Yu, Z. Z., Feng, Y. J., Xu, X. F., Zhao, J. M. & Jiang, T. Optimized cylindrical invisibility cloak with minimum layers of non-magnetic isotropic materials. *J. Phys. D: Appl. Phys.* **44**, 185102 (2011).
19. Yu, Z. Z., Yang, Z., Wang, Y. H., Si, H. F. & Zhao, G. S. Optimized cloaks made of near-zero materials for different-sized concealed targets. *Sci. Rep.* **8**, 16739 (2018).
20. Bohren, C. F. & Huffmann, D. R. Absorption and scattering of light by small particles. Wiley, New York (1983).
21. Winter, G. Genetic algorithms in engineering and computer science. J. Wiley, New York (1995).

Acknowledgements

This work is supported by the Research Foundation of Jinling Institute of Technology (Grant No. JIT-B-202029, No. JIT-B-201628 and No. JIT-fhxm-201906) and Modern Technology Education Research Project of Jiangsu Province (No. 2019-R-80918).

Author contributions

Z. Z. Y. and Y. Z. conceived the idea and conducted the theoretical calculation. Z. Y. and X. L. H. performed the numerical simulation and data analysis. All authors discussed the results and contributed to the writing of the manuscript. Y. Z. W. and X. M. T. carefully revised the manuscript before the submission.

Additional information

Competing interests: The authors declare no competing interests.

Figures

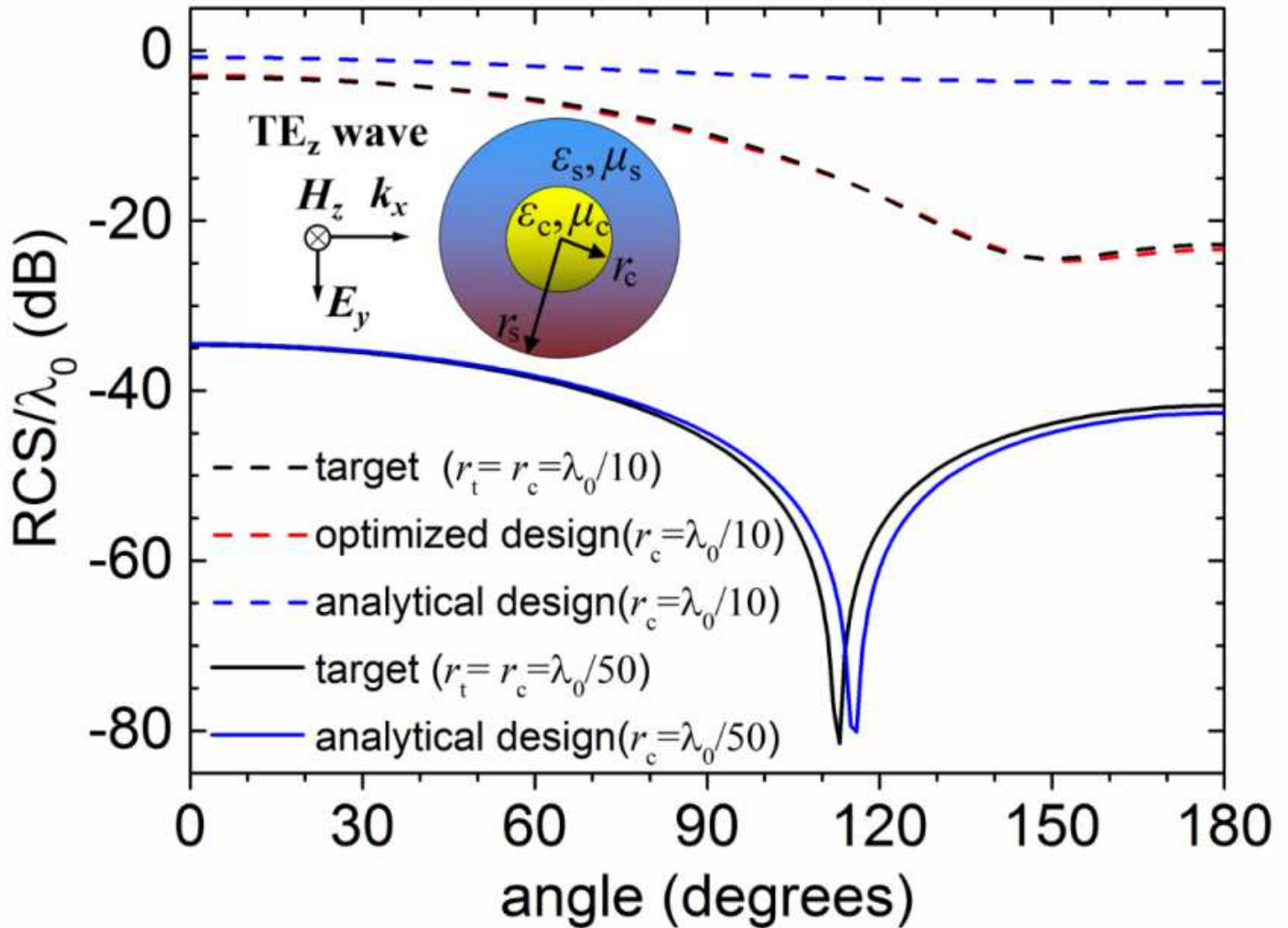


Figure 1

The scattering width normalized by wavelength for the optimized and analytical core-shell design. Two different radii of the core are considered respectively with $r_c = \lambda_0/10$ (dashed lines) and $r_c = \lambda_0/50$ (solid lines). We assume that the radii of core and target are equal, namely $r_t = r_c$. The constitutive parameters of the core and the target are $(3\epsilon_0, 3\mu_0)$ and $(5\epsilon_0, 1.5\mu_0)$, respectively. The inset shows that a TE_z plane wave is normally incident on a core cylinder coated by a homogeneous isotropic shell.

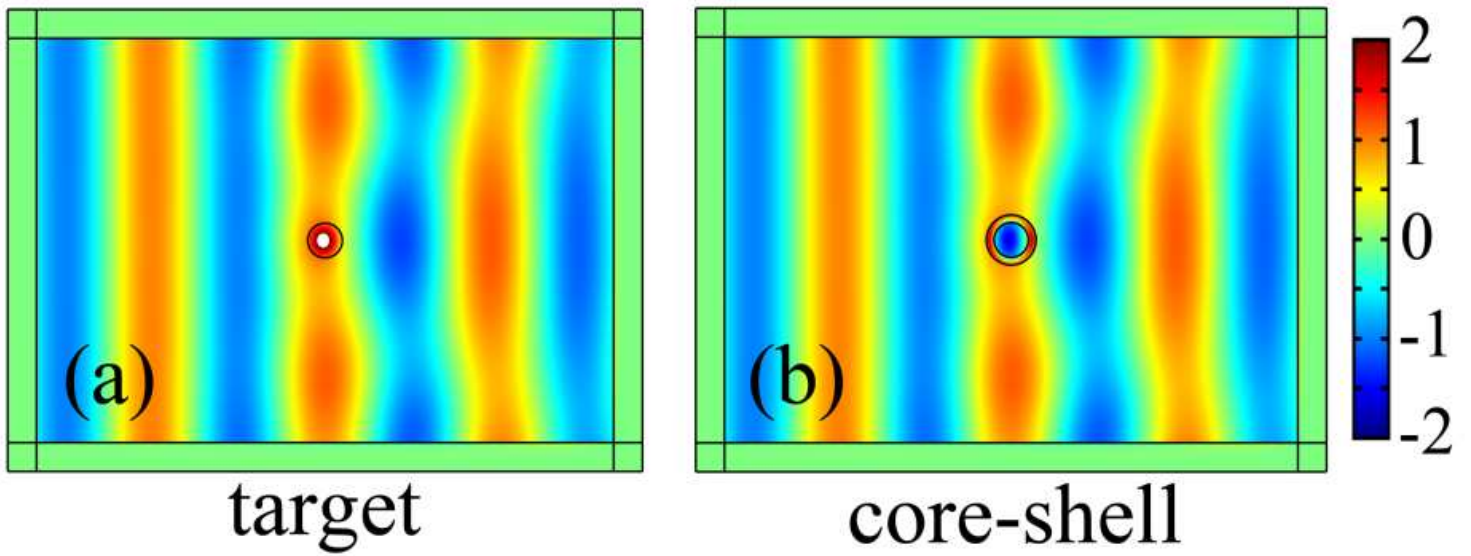


Figure 2

A TE_z polarized plane wave with unit magnitude is incident horizontally from the left side. The z-directed magnetic field distributions of the target (a) and the optimized core-shell illusion device (b) are simulated using COMSOL Mutiphysics. The magnitudes out of the colour bar range are represented by white area.

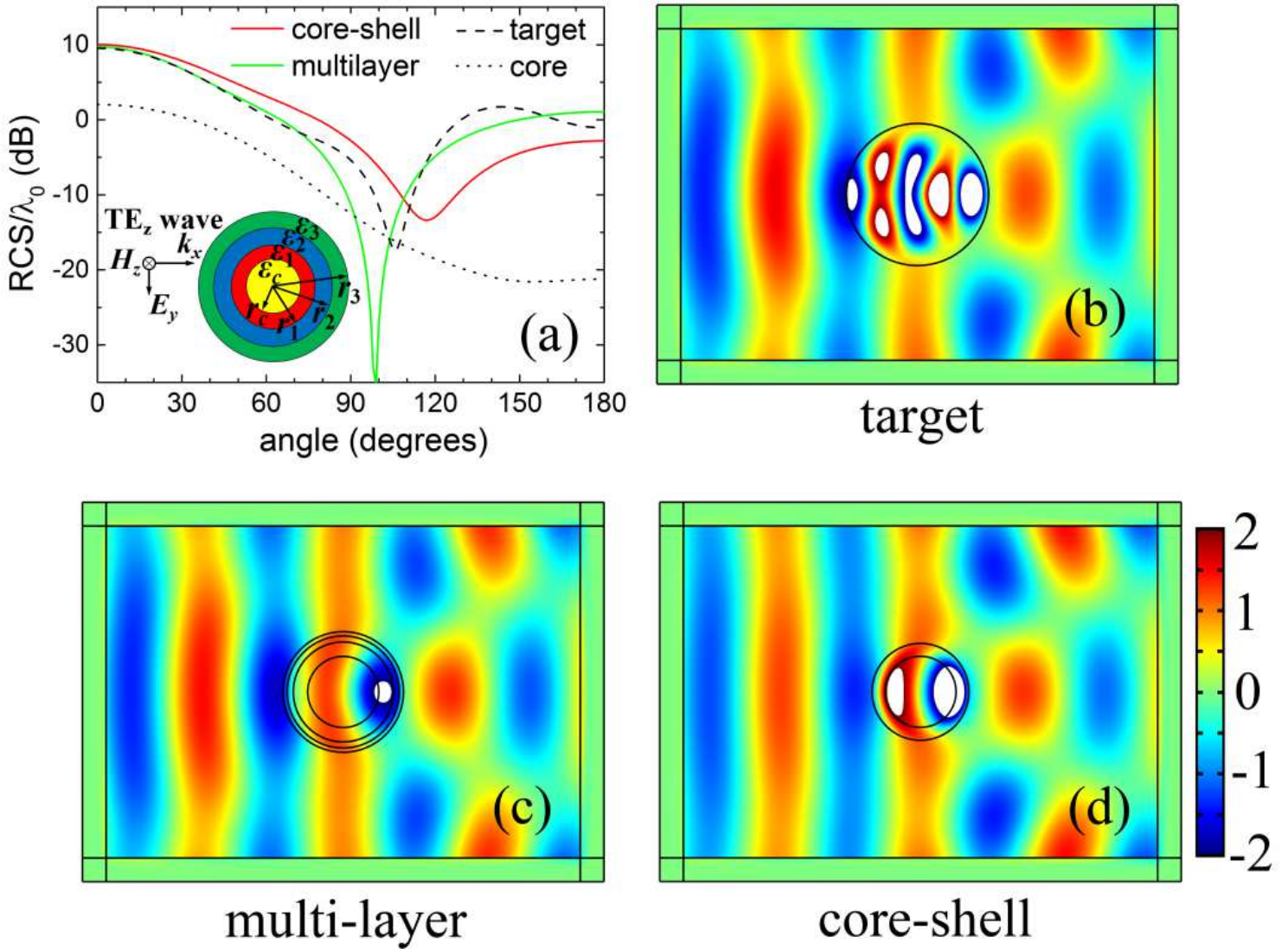


Figure 3

(a) The scattering width normalized by wavelength for the target cylinder with radius $r_t = \lambda_0/2$ (dashed black line), the core cylinder with radius $r_c = \lambda_0/4$ (dotted black line), the optimized multi-layered design (solid green line), and the optimized core-shell design (solid red line). The inset shows that a core cylinder coated by three layers of homogeneous and isotropic materials. The magnetic field distributions of the target (b), the optimized multi-layered illusion device (c), and the optimized core-shell illusion device (d) are simulated using COMSOL Mutiphysics. The magnitudes out of the colour bar range are represented by white area.

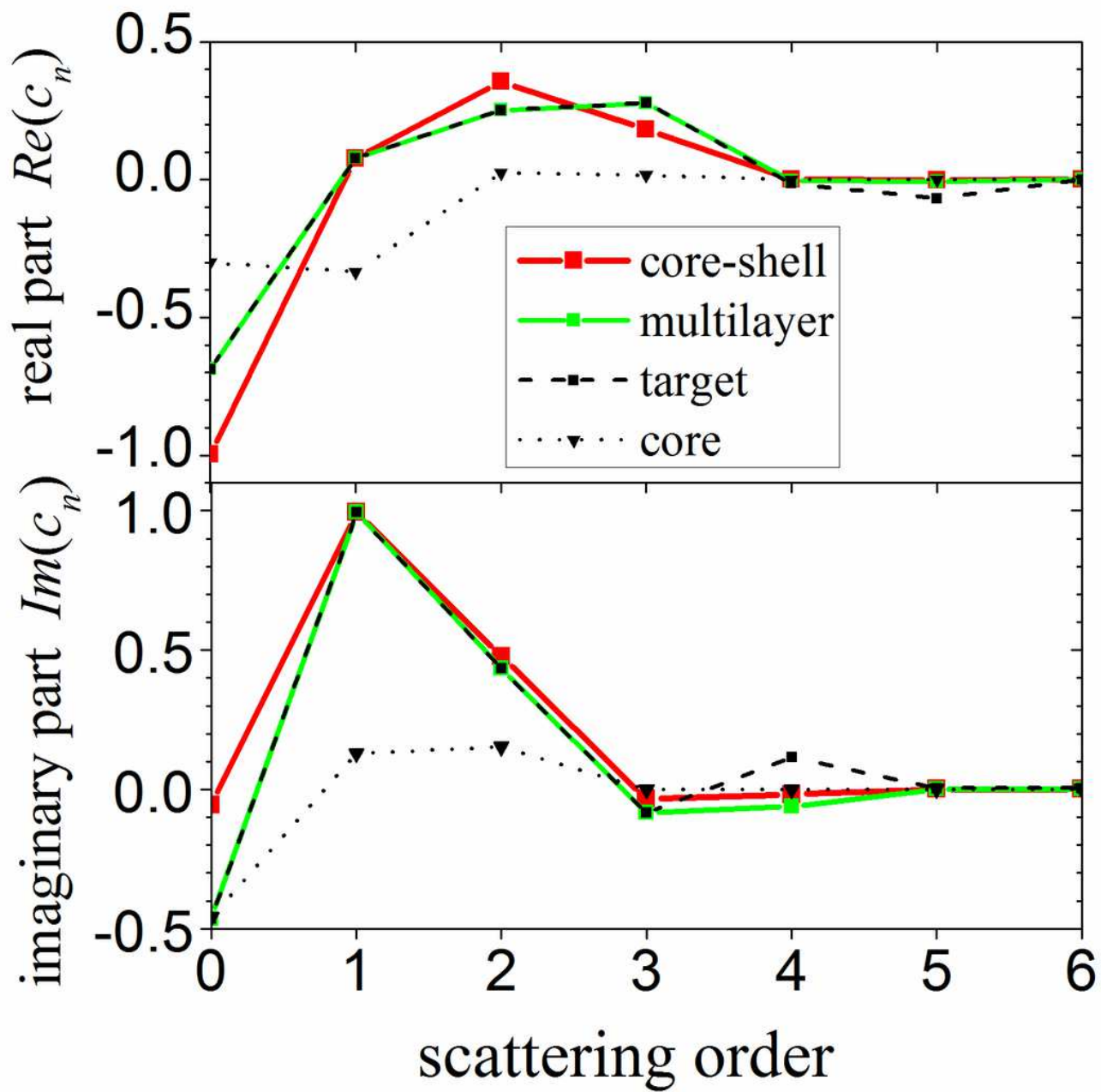


Figure 4

Real and imaginary parts of the Mie scattering coefficients for the optimized 3-layer illusion device at different scattering orders.